Proceedings of the 3rd IASME/WSEAS Int. Conf. on HEAT TRANSFER, THERMAL ENGINEERING AND ENVIRONMENT, Corfu, Greece, August 20-22, 2005 (pp184-190)

Wall Oscillation Effects on Heat Convection in a Rectangular Enclosure

Kuo-Shu Hung* Chin-Hsiang Cheng†
Department of Mechanical Engineering
Tatung University
40 Chungshan North Road, Sec. 3
Taipei, Taiwan 10451
Republic of China

Abstract: Effects of wall vibration on natural convection in a rectangular enclosure containing air are investigated in this report. In practical applications, the wall vibration driven by an external force leads to periodic variations in the flow and thermal fields within the rectangular enclosure, and hence results in different features from those in a stationary enclosure. Two types of thermal boundary condition are considered, involving a heated-vertical-walls and a heated-horizontal-walls situations. The solution method is based on a two-stage pressure correction scheme, which is applied to determine the absolute pressure, density, temperature, and velocity components of the compressible flow in enclosures. The vibration frequency of the wall is varied from 1 to 50 Hz and the vibration amplitude is ranged between 1.4 and 5.6 percent enclosure length. In this study, Rayleigh number is fixed at 10^5. For the parameter ranges considered, results show that a maximum 700 % fluctuation in heat transfer is attained due to the wall vibration.

Key-Words: wall oscillation, vibration, rectangular enclosure, numerical solution, convection

1 Introduction

Natural convection in the enclosures with different thermal boundary conditions has commonly been predicted by using numerical methods. For example, Pepper and Hollands [1] presented a numerical study for the three-dimensional natural convection characteristics in an enclosure inclined at three different angles and at four different Rayleigh numbers. Benchmark solutions for heat transfer rate of two-dimensional or three-dimensional flow and natural convection in the enclosures were reviewed by de Vahl Davis and Jones [2]. It is recognized that the physical models presented in the exiting reports are simplified to be stationary systems with fixed walls. To the authors' knowledge, the effects of wall vibration were not taken into consideration in the existing reports. However, in practical applications, the enclosure may be brought into vibration by external forces. For example, in an electronic device equipped with a fan-cooled module, wall vibration may be caused from the fan motor, and the vibration of the wall leads to a significant change in the features of the momentum and thermal boundary layers along the walls. Unfortunately, the effects of wall vibration on natural convection heat transfer in the enclosures are not sufficiently discussed so that the related information is still lacking.

Analysis of the flow and thermal behavior in an enclosure with vibrating wall may be categorized to moving-boundary problems. The moving-boundary problems may be encountered in a variety of applications. Fu, Ke, and Wang [3] investigated laminar forced convection in a parallel-plate channel with an oscillating block. They found that the movement of the block leads to a remarkable increase in heat transfer on the channel surfaces. Fu and Shieh [4] simulated the effects of vertical vibration and gravity on the induced thermal convection in the enclosure by adding additional terms into the momentum equations. By authors of Refs.[3,4] it has been concluded that the vibration of the walls or the object in the enclosure space may play a subtle role in heat transfer enhancement.

The flow problems associated with vibrating walls are usually solved by adopting an inertial or alternatively a non-inertial reference frame. These problems adopting inertial reference frame feature a boundary movement, and hence they are in essence more involved in dealing with the boundary conditions than the problems using the non-inertial reference frame. For example, Cheng, Hong, and Aung [5] used a non-inertial reference frame to study the cross flow over an oscillating cylinder. Using this method, authors are able to avoid the complexity caused by moving boundary with the method using

inertial frame. On the other hand, Hirt, Amsden and Cook [6] proposed an arbitrary Lagrangian-Eulerian scheme with the inertial reference frame based on a grid of which the vertices may move with the boundary, be held fixed, or move in any other prescribed way. Such a scheme leads to a fair assessment of the flow and thermal behavior in the enclosure with vibrating wall, but requires more efforts in dealing with the dynamic grid deformation. As a matter of fact, in the past several decades, a number of reports dealing with the deforming grids have been presented for different applications. Demirdzic and Peric [7] extended the capability of numerical predictions of the moving-boundary flows to the problems with a domain of irregular shape. Gosman [8] developed an RPM method for predicting in-cylinder processes within a reciprocating internal-combustion engine based on $k-\varepsilon$ turbulence model and related wall functions. Lately, Kelkar and Patankar [9] investigated changes of free surfaces between liquid water and air contained in a piston-cylinder assembly during the compression process. Their study was focused on the development of a computational method using a combination of the deforming grid and the volume-of-fluid technique [10].

In the space of an enclosure with vibrating walls, the fields of velocity, absolute pressure, temperature, and density were periodically varied due to the wall vibration. Since these physical variables are dependent on each other, without simultaneous solution for these variables at each time instant the results obtained may not reflect the real phenomenon taking place in the solution domain. Therefore, in an earlier report, Cheng and Hung [11] proposed a two-stage pressure correction method in order to pursue the simultaneous solutions for temperature, density, absolute pressure and velocity. This solution method was based on the finite-volume method with a deforming staggered grid system, it has been proven efficient and stable when it is applied for the problems with vibrating walls.

In these circumstances, in the present study, the two-stage pressure correction method [11] is extended to the applications in seeking the solution for natural convection in an enclosure with a vibrating wall. Two types of thermal boundary conditions commonly encountered are considered to evaluate the effects of wall vibration on the flow and temperature fields, which are a heated-vertical-walls and a heated-horizontal-walls situations.

Physical model of a rectangular enclosure with a vibrating wall is shown in Fig.1. The enclosure is square of length *H*. The right vertical wall of the enclosure is brought to a vibration by an external

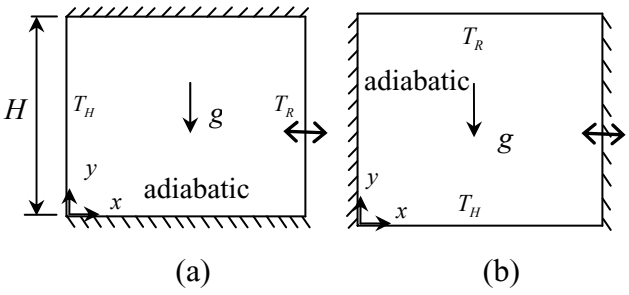

Fig.1 A square enclosure with a vibrating wall.
(a) heated-vertical-walls situation
(b) heated-horizontal-walls situation

force between the bottom-dead (BDP) and the top-dead points (TDP). The time-dependent location of the right wall x_{vib} can be expressed as

$$x_{vib}(t) = (\frac{l_B + l_T}{2}) + \frac{l}{2}\sin(2\pi ft) \tag{1}$$

where *f* represents the vibration frequency of the wall, l_B and l_T indicate the positions of the BDP and TDP, respectively, and l denotes the stroke of the vibration which is equal to $l_B - l_T$. The vibration stroke is two times amplitude in length.

The steady-state solutions associated with the stationary systems with fixed walls are adopted as initial conditions for the corresponding vibrating-wall cases. In this study, the vibration stroke of the wall is ranged between 1.4 and 5.6 percent enclosure length.

2 Theoretical analysis

The air in the enclosure with a vibrating wall is assumed to be compressible, homogeneous, and isotropic, and the work done by the gravity and the viscous forces are neglected. The conservation statements of space, mass, momentum, and energy in dimensionless integral forms are :

$$\frac{d}{d\tilde{t}}\int_{cv} d\tilde{\forall} = \int_{cs} \tilde{\vec{V}}_b \cdot d\tilde{\vec{A}} \tag{2}$$

$$\frac{d}{d\tilde{t}}\int_{cv} \tilde{\rho} d\tilde{\forall} = -\int_{cs} \tilde{\rho}(\tilde{\vec{V}} - \tilde{\vec{V}}_b) \cdot d\tilde{\vec{A}} \tag{3}$$

$$\frac{d}{d\tilde{t}}\int_{cv}\tilde{\rho}\tilde{u}d\tilde{V}=-\int_{cs}\tilde{\rho}\tilde{u}(\tilde{\vec{V}}-\tilde{\vec{V}}_b)\cdot d\tilde{\vec{A}}-\int_{cv}(\nabla\tilde{P}\cdot\vec{i})d\tilde{V}+\int_{cs}\tilde{\vec{t}}_x\cdot d\tilde{\vec{A}} \quad (4)$$

$$\frac{d}{d\tilde{t}}\int_{cv}\tilde{\rho}\tilde{v}d\tilde{V}=-\int_{cs}\tilde{\rho}\tilde{v}(\tilde{\vec{V}}-\tilde{\vec{V}}_b)\cdot d\tilde{\vec{A}}-\int_{cv}(\nabla\tilde{P}\cdot\vec{j})d\tilde{V}+\int_{cs}\tilde{\vec{t}}_y\cdot d\tilde{\vec{A}}-B\int_{cv}(\tilde{\rho}-\tilde{\rho}_E)d\tilde{V} \quad (5)$$

$$\frac{d}{d\tilde{t}}\int_{cv}\tilde{\rho}\tilde{T}d\tilde{V}=C_1\frac{d}{d\tilde{t}}\int_{cv}\tilde{P}d\tilde{V}-\int_{cs}\tilde{\rho}\tilde{T}(\tilde{\vec{V}}-\tilde{\vec{V}}_b)\cdot d\tilde{\vec{A}}-\int_{cs}\tilde{\vec{q}}\cdot d\tilde{\vec{A}}-C_1\int_{cs}\tilde{P}\tilde{\vec{V}}_b\cdot d\tilde{\vec{A}}+C_2\frac{d}{d\tilde{t}}\int_{cv}\tilde{P}_E d\tilde{V}-C_2\int_{cs}\tilde{P}_E\tilde{\vec{V}}_b\cdot d\tilde{A} \quad (6)$$

These above dimensionless parameters are defined by

$$\tilde{x}=\frac{x}{H},\ \tilde{y}=\frac{y}{H},\ \tilde{t}=\frac{tU_R}{H},\ \tilde{\rho}=\frac{\rho}{\rho_R},\ \tilde{\rho}_E=\frac{\rho_E}{\rho_R},\ \tilde{u}=\frac{u}{U_R},\ \tilde{v}=\frac{v}{U_R},\ \tilde{T}=\frac{T}{T_R},\ \tilde{P}=\frac{P-P_E}{\rho_R U_R{}^2},\ \tilde{P}_E=\frac{P_E}{\rho_R RT_R},\ B=\frac{gH}{U_R{}^2},\ C_1=\frac{U_R{}^2}{C_P T_R},\ C_2=\frac{R}{C_P}$$

where U_R , ρ_R , and T_R are the characteristic velocity, density, and temperature, which are given by U_R =πfl, ρ_R =1.20 kg/m^3 and T_R =303 K, respectively, and $\tilde{\vec{t}}_x=[\tilde{\tau}_{ij}]\cdot\vec{i}$, $\tilde{\vec{t}}_y=[\tilde{\tau}_{ij}]\cdot\vec{j}$, with $[\tilde{\tau}_{ij}]$ the stress tensor.

Recall that at t=0, $T=T_R$, $P=P_E$, and $\rho=\rho_E$. With the help of the dimensionless ideal-gas equation

$$\tilde{\rho}=\frac{C\tilde{P}+\tilde{P}_E}{\tilde{T}} \quad (7)$$

where $C=C_1/C_2$, one has

$$\tilde{P}_E=\tilde{\rho}_E=e^{-\frac{gH}{RT_R}\tilde{y}}=e^{-F\tilde{y}} \quad (8)$$

where $F=gH/RT_R$. Using Eq.(8), the values of $\tilde{P}_E$ and $\tilde{\rho}_E$ appearing in Eqs.(5) and (6) can be calculated.

Boundary and initial conditions for the test problem can be given as:

$$\tilde{u}=\frac{d\tilde{x}_{pis}}{d\tilde{t}},\ \tilde{v}=0 \text{ on piston surface at } \tilde{x}=\tilde{x}_{pis}(\tilde{t}) \quad (9a)$$

$$\tilde{u}=\tilde{v}=0 \quad \text{on cylinder surfaces} \quad (9b)$$

$$\tilde{T}=1 \quad \text{on all surfaces} \quad (9c)$$

$$\tilde{u}=\tilde{v}=0,\ \tilde{T}=1,\ \tilde{\rho}=\tilde{\rho}_E=e^{-F\tilde{y}}, \text{ and } \tilde{P}=0 \text{ at } \tilde{t}=0 \quad (9d)$$

3 Numerical Methods

In the present study, the moving grid lines divide the periodically-varied solution domain into a fixed number of control cells whose volumes change with time. A staggered grid system is adopted herein. Typically, computation is carried out with 53×53 grids. The magnitude of $\Delta\tilde{t}$ would have to be sufficiently small so that the Courant number ($\Delta\tilde{t}\tilde{u}_b/\Delta\tilde{x}$) will be much less than unity. Therefore, $\Delta\tilde{t}$ is chosen to ensure the satisfaction with this condition. Discretization forms of the integral governing equations are carried out on the staggered grids. The velocities of the moving cell faces are prescribed so that the change in the volume of the solution domain is absorbed equally by all cells. The space conservation law is used to determine the velocities of the faces for the staggered cells. For example, based on Eq.(1), one obtains

$$\tilde{u}_{b,e}=\tilde{u}_{b,w}+\frac{\tilde{x}_{vib}(\tilde{t}+\Delta\tilde{t})-\tilde{x}_{pis}(\tilde{t})}{N\Delta\tilde{t}} \quad (10)$$

where $\tilde{u}_{b,e}$ and $\tilde{u}_{b,w}$ are the dimensionless velocities of faces e and w of the main cell, respectively. N is the number of main grid points in the x-direction.

The tentative mass at each step is calculated and the density field is updated by introducing the updated absolute pressure until the requirement of the mass conservation is fulfilled. That is,

$$\left| \tilde{m}^* - \tilde{m} \right| = \left| \iint \tilde{\rho}(\tilde{P}^{*n} + \tilde{P}_0, \tilde{T}) d\tilde{x} d\tilde{y} - \tilde{m} \right| \le \varepsilon \quad (11)$$

In this study, the value of ε is assigned to be 10^{-9}. The discretization equations of these equations are solved by using the two-stage pressure correction method proposed by Cheng and Hung [11]. Detailed information for the numerical methods can be found in Ref. [11].

4 Results and Discussion

Numerical predictions of temperature distribution are used to determine local or average heat transfer coefficients on the isothermal walls. The average heat transfer coefficient is

$$\bar{h} = -\frac{k}{H(T_H - T_R)} \int_0^H \left. \frac{\partial T}{\partial x} \right|_{x=0, x_{vib}} dy \quad (12a)$$

or

$$\bar{h} = -\frac{k}{x_{vib}(T_H - T_R)} \int_0^{x_{vib}} \left. \frac{\partial T}{\partial y} \right|_{y=0, H} dx \quad (12b)$$

As long as the average heat transfer coefficient is obtained, the Nusselt number at the isothermal walls given by

$$Nu = \frac{\bar{h}H}{k} \quad \text{(on vertical walls)} \quad (13a)$$

or

$$Nu = \frac{\bar{h}x_{vib}}{k} \quad \text{(on horizontal walls)} \quad (13b)$$

can be determined.

Numerical solutions are carried out for a number of test cases. The variables of the cases discussed in this study are listed in Table 1.

Figure 2 shows the transient variations of the dimensionless variables, $\tilde{P}$, $\tilde{T}$, $\tilde{u}$ and $\tilde{v}$ for case 1 described in Table 2. In the plots of this figure, data for the grid point specified at $(\tilde{x}, \tilde{y}) = (0.28\tilde{x}_{vib}, 0.28)$ are displayed. It is observed that all dimensionless variables exhibit a periodically stable feature after a finite number of cycles from the initial steady-state solution. The vertical component of the velocity $\tilde{v}$ is relatively small and exhibits a two-frequencies oscillatory feature. The higher frequency is identical to the wall vibration frequency, whereas the lower-frequency oscillation is repeated per seven cycles. However, for the horizontal velocity component $\tilde{u}$, the lower-frequency oscillation is not appreciable, relatively.

Table 1 Test cases

Case	Thermal boundary	Frequency f [Hz]	Stroke L(l/H)
1	Heated-vertical	1	0.028
2	Heated-horizontal	1	0.028
3	Heated-vertical	50	0.028
4	Heated-horizontal	50	0.028
5	Heated-vertical	1	0.014
6	Heated-vertical	1	0.056
7	Heated-horizontal	1	0.014
8	Heated-horizontal	1	0.056
9	Heated-vertical	50	0.014
10	Heated-horizontal	50	0.014
11	Heated-vertical	50	0.056
12	Heated-horizontal	50	0.056

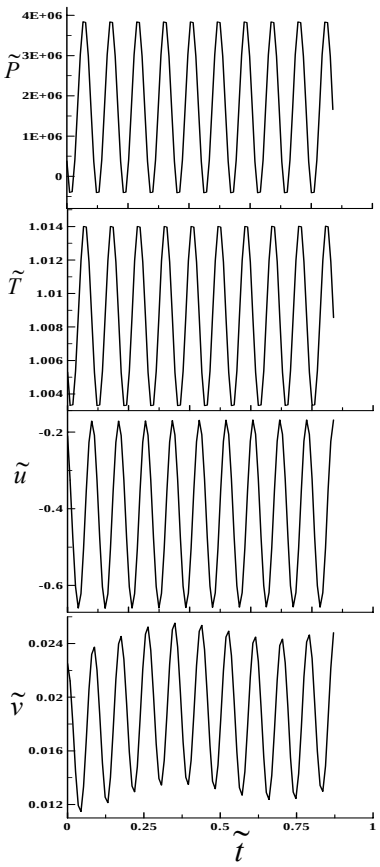

Fig.2 Variations of dimensionless quantities for case 1 for the first ten cycles. All values are taken at the point of $\tilde{x} = 0.28\tilde{x}_{vib}$ and $\tilde{y} = 0.28$.

In order to have a deeper insight of the cyclic variations in the flow and the thermal fields caused by the vibration of the right wall, a number of snapshots of the velocity and the temperature distributions in a cycle in the stable regime for cases 1 and 3 are show in Fig.3. The vibration frequencies of cases 1 and 3 are 1 and 50 Hz, respectively, such that the influence of vibration frequency can also be observed. The flow field is illustrated by plotting the velocity vectors, and the thermal field by plotting the isotherms. In the cyclic process, it is found that the temperature distribution in the enclosure space is appreciably altered by the variation of the right wall for all the cases.

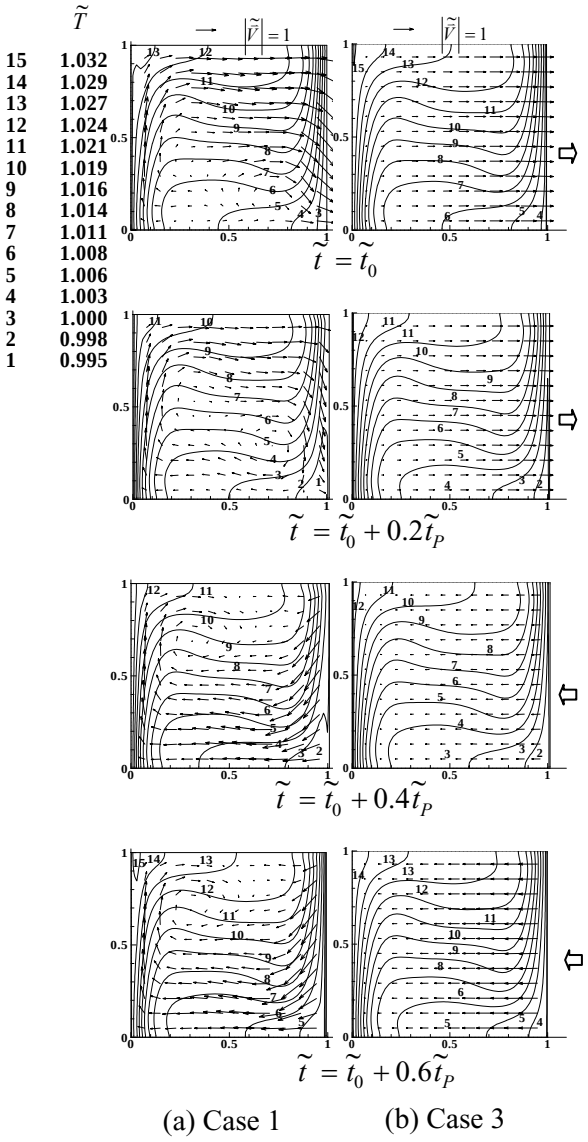

(a) Case 1 (b) Case 3

Fig.3 Snapshots of velocity and temperature distributions in a cycle in the stable regime for cases 1, and 3.

The fluid temperature is increased during the compression process and decreased during the expansion process. The dimensionless temperature ($\widetilde{T}$) reaches a maximum of 1.032 due to compression for case 1. The thermal field experiences a remarkable change as the vibration frequency is elevated. On the other hand, the velocity distribution is also greatly influenced by the back-and-forth movement of the right wall. For a lower-frequency case (case 1), the flow in the enclosure is driven mainly by the buoyancy. The fluid in the area adjacent to the hotter left wall moves upwards and that adjacent to the colder right wall moves downwards. Therefore, a flow recirculation is formed in the enclosure. The location of the center of the flow recirculation is not steady but varied with time. As the vibration frequency is increased to be 10 Hz or greater, the flow in the enclosure is dominated by the inertia effects from the movement of the vibration wall; therefore, it is clearly seen that for the high-frequency cases, the velocity vectors of the fluid is nearly in resonance with the wall vibration velocity

When the thermal boundary condition is changed, different flow and thermal characteristics are observed. Fig. 4 shows the variations in velocity and temperature distributions in the stable regime for the heated-horizontal-walls situation at f =1 and 50 Hz (that is, for cases 2 and 4, respectively). The dependence of the temperature distribution on the vibration frequency can be observed. A large flow recirculation is produced in the enclosure at low vibration of f =1 Hz. It is noted that at f =0, which indicates no wall vibration, two symmetric and stable fluid vortices were observed in the enclosure under pure free convection situation. The symmetric pattern was significantly shifted to an asymmetric pattern with a flow recirculation due to the wall vibration even at f = 1 Hz. The flow recirculation moves vortices move up-and-down accompanying the movement of the right wall. The local density of the isotherms adjacent to the horizontal walls is lower at f = 1 Hz than at f = 50 Hz. This implies that the thermal boundary layers are thicker and hence the heat transfer rate on the horizontal walls is lower at f = 1 Hz. Again, as the vibration frequency is increased to be 50 Hz, the flow recirculation is not visible. The fluid oscillation caused by wall vibration can be observed in Fig.5 for case 3. In this figure, the dimensionless velocity component $\widetilde{u}$ at different positions in the enclosure are plotted. The monitored positions are located at x/H = 0.25, 0.5, and 0.96 x_{vib}/H and y/H = 0.5. It is found that the dependence of the fluid oscillation on the wall vibration is more

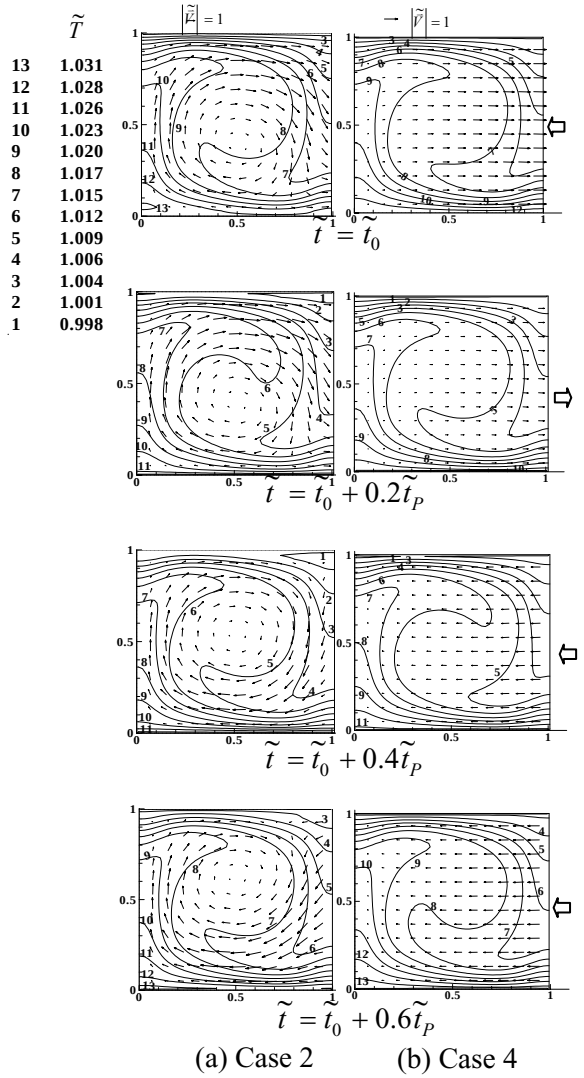

(a) Case 2 (b) Case 4

Fig.4 Snapshots of velocity and temperature distributions in a cycle in the stable regime for cases 2 and case 4.

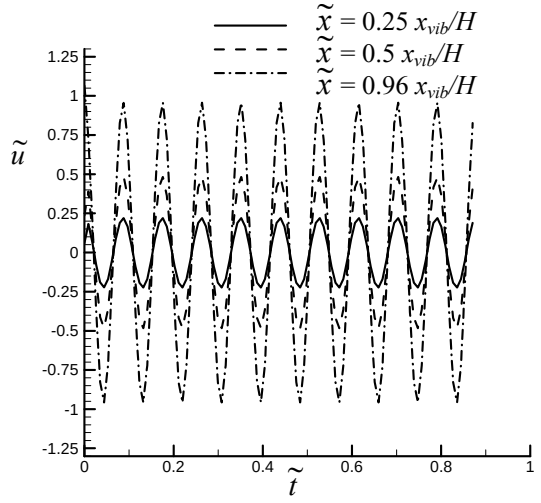

Fig.5 Oscillation of $\tilde{u}$ for the points at different positions in x-direction at $\tilde{y} = 0.5$, for case 3.

significant for the points closer to the vibrating wall. For the points in the immediate neighboring area of the vibration wall, the local fluid velocity is nearly identical to that of the vibration wall. The frequencies of the fluid oscillation at the three positions are all equal; however, the amplitude of the fluid oscillation is a function of the distance from the vibrating wall.

Fig. 6 shows the variations in average Nusselt numbers in the first ten cycles for different combinations of frequency and amplitude in the heated-vertical-walls situation. Both the Nusselt number data on the hot and cold walls are plotted with solid and dashed curves, respectively. The mean value of the time-varying Nu is only slightly increased by the wall vibration, as compared with that of the stationary enclosure with fixed walls. However, it is found that in the heated-vertical-walls situation the magnitude of the fluctuation of average Nusselt number is increased with frequency and

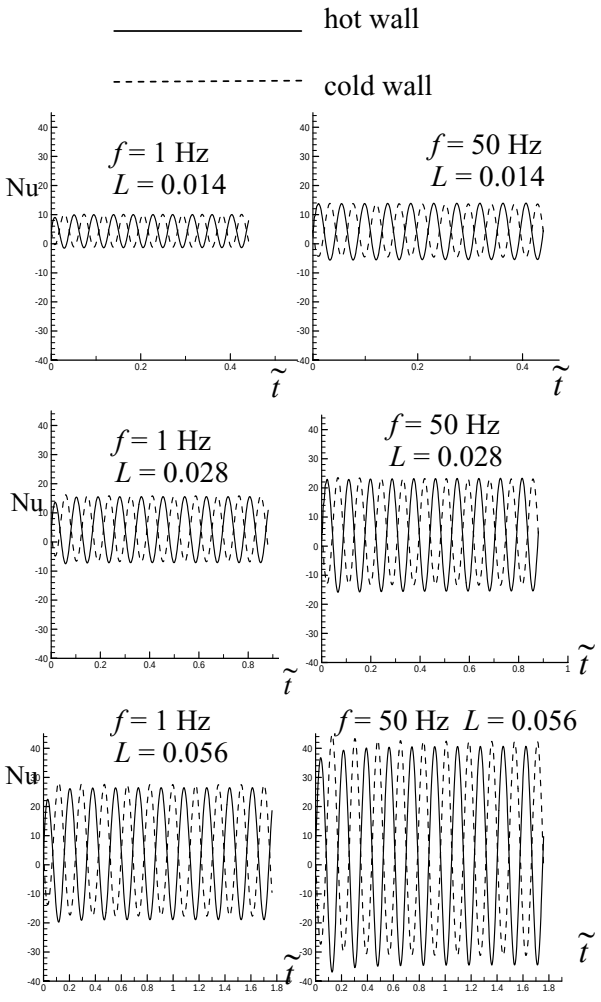

Fig.6 Variations in average Nusselt numbers in the first ten cycles for heated-vertical-walls situation.

amplitude of wall vibration. For the case with f = 50 Hz and L = 0.056, the fluctuation of Nu reaches approximately 34.0, which means that 700 % fluctuation in heat transfer rate may be caused by wall vibration. It is noted that for the heated-horizontal-walls situation, the dependence of Nu on the frequency and amplitude is similar to that of the heated-vertical-walls situation.

5 Conclusion

In this study, the effects of wall vibration on natural convection in a rectangular enclosure are presented. The vibrating wall leads to periodic variations in the flow and thermal fields within the rectangular enclosure, and hence results in different features from those in a stationary enclosure. Two types of thermal boundary condition are considered, involving a heated-vertical-walls and a heated-horizontal-walls situations. The vibration frequency of the wall is varied from 1 to 50 Hz and the vibration stroke is ranged between 1.4 and 5.6 percent enclosure length.

Results show that an unsteady flow recirculation is formed and varied with time for the lower-frequency situation. Then, the thermal field experiences a remarkable change as the vibration frequency is elevated. The velocity vectors of the fluid is nearly in resonance with the wall vibration velocity for the high-frequency cases.

The data of average Nusselt numbers show no remarkable difference in the dependence on wall oscillation between the two types of thermal boundary conditions. For both situations, the magnitude of the fluctuation of the average Nusselt number is increased with frequency and amplitude of wall vibration. For the case with f = 50 Hz and L = 0.056, the fluctuation of Nu reaches approximately 34.0, which means that a 700 % fluctuation in heat transfer rate may be caused by wall vibration.

References:

[1] D. W. Pepper, and K. G. T. Hollands, Summary of Benchmark Numerical Studies for 3-D Natural Convection in an Air-Filled Enclosure, *Numerical Heat Transfer*, Part A. Vol.42, 2002, pp.1-11.

[2] G. de Vahl Davis and I. P. Jones, Natural Convection in a Square cavity: a Comparison Exercise, *Int. J. Numerical Methods in Fluids*, 3, 1983, pp.227- 248.

[3] W.S. Fu, W.W. Ke, and K.N. Wang, Laminar Forced Convection in a Channel With a Moving Block, *Int. J. Heat Mass Transfer*, Vol. 44, 2001, pp.2385-2394.

[4] W. S. Fu, and W. J. Shieh, A study of Thermal Convection in An Enclosure Induced Simultaneously by Gravity and Vibration, Int. J. Heat Mass Transfer, Vol.35, 1992, pp.1965-1710.

[5] C. H. Cheng, J.L. Hong, and W. Aung, Numerical Prediction of Lock-on Effect on Convective Heat Transfer From a Transversely Oscillating Circular Cylinder, *Int. J. Heat Mass Transfer*, Vol. 40, 1997, pp.1825-1834.

[6] C. W. Hirt, A. A. Amsden, and J. L. Cook, An Arbitrary Lagrangin-Eulerian Computing Method for All Flow Speeds, Journal of Computational Physics, Vol.14, 1974, pp.227-253.

[7] I. Demirdzic and M. Peric, Finite Volume Method for Prediction of Fluid Flow in Arbitrarily Shaped Domains with Moving Boundary, Int. J. *Numerical Methods in Fluids*, Vol.10, 1990, pp. 771-790.

[8] A. D. Gosman, Prediction of In-Cylinder Process in Reciprocating Internal Combustion Engines, *in Computer Methods in Applied Science and Engineer* (editors : R. Glowinski and J. L. Lions), Elsevier, Amsterdam, 1984, pp.609-629.

[9] K. M. Kelkar and S. V. Patankar, Numerical Method for the Prediction of Free Surface Flow in Domains with Moving Boundaries, *Numerical Heat Transfer*, Part B, Vol.31, 1997, pp.387-399.

[10] C.W. Hirt and B.D. Nichols, Volume of Fluid (VOF) Method for the Dynamics of Free Boundaries, *J. Computational Physics*, Vol.39, 1981, pp.201-225.

[11] C. H. Cheng, and K. S. Hung, Numerical Predictions of Flow and Thermal Fields in a Reciprocating Piston-Cylinder Assembly, *Numerical Heat Transfer*, Part A, Vol.38, 2000, pp.397-421.